Journal of Infection and Public Health 16 (2023) 1368–1378

Contents lists available at ScienceDirect

Journal of Infection and Public Health

journal homepage: www.elsevier.com/locate/jiph

Original article

Novel mutations in genes of the IL-12/IFN-γ axis cause susceptibility to tuberculosis

Sajjad Ahmad [a,1], Jawad Ahmed [b,2], Eman H. Khalifa [c,3], Farhad Ali Khattak [d,4], Anwar Sheed khan [e,5], Syed Umar Farooq [f,6], Sannaa M.A. Osman [g,7], Magdi M. Salih [h,8], Nadeem Ullah [i,*,9], Taj Ali Khan [b,j,**]

[a] Institute of Basic Medical Science, Khyber Medical University, Peshawar, KP, Pakistan
[b] Institute of Pathology and Diagnostic Medicine, Khyber Medical University, Peshawar, Pakistan
[c] Al Baha University Faculty of Applied Medical Sciences, Saudi Arabia
[d] Research & development Cell, Khyber College of Dentistry (KCD), Peshawar, Pakistan
[e] Provincial TB Reference laboratory, Hayatabad Medical Complex, Peshawar, PK, Pakistan
[f] Department of oral pathology, Khyber College of Dentistry, Peshawar. Pakistan
[g] Alzaiem Alazhari University Faculty of Medicine, Sudan
[h] Taif University College of Science, Saudi Arabia
[i] Department of Clinical Microbiology, Umeå University, 90185 Umeå, Sweden
[j] Division of Infectious Diseases & Global Medicine,Department of Medicine,University of Florida, Gainesville, FL,United States

ARTICLE INFO

Article history:
Received 9 March 2023
Received in revised form 15 May 2023
Accepted 6 June 2023

Keywords:
TB
PBMCs
IL-12Rβ1
NEMO
CYBB
IFN-γ

ABSTRACT

Background: The IL-12/23/ISG15-IFN-γ pathway is the main immunological pathway for controlling intra-macrophagic microorganisms such as *Mycobacteria*, *Salmonella*, and *Leishmania spp*. Consequently, upon mutations in genes of the IL-12/23/ISG15-IFN-γ pathway cause increased susceptibility to intra-macrophagic pathogens, particularly to *Mycobacteria*. Therefore, the purpose of this study was to characterize the mutations in genes of the IL-12/23/ISG15-IFN-γ pathway in severe tuberculosis (TB) patients.
Methods: Clinically suspected TB was initially confirmed in four patients (P) (P1, P2, P3, and P4) using the GeneXpert MTB/RIF and culturing techniques. The patients' Peripheral blood mononuclear cells (PBMCs) were then subjected to ELISA to measure Interleukin 12 (IL-12) and interferon gamma (IFN-γ). Flow cytometry was used to detect the surface expressions of IFN-γR1 and IFN-γR2 as well as IL-12Rβ1and IL-12Rβ2 on monocytes and T lymphocytes, respectively.The phosphorylation of signal transducer and activator of transcription 1(STAT1) on monocytes and STAT4 on T lymphocytes were also detected by flow cytometry. Sanger sequencing was used to identify mutations in the *IL-12Rβ1, STAT1, NEMO,* and *CYBB* genes.
Results: P1's PBMCs exhibited reduced IFN-γ production, while P2's and P3's PBMCs exhibited impaired IL-12 induction. Low IL-12Rβ1 surface expression and reduced STAT4 phosphorylation were demonstrated by P1's T lymphocytes, while impaired STAT1 phosphorylation was detected in P2's monocytes. The impaired IκB-α degradation and abolished H2O2 production in monocytes and neutrophils of P3 and P4 were observed, respectively. Sanger sequencing revealed novel nonsense homozygous mutation: c.191 G > A/p.W64 * in exon 3 of the *IL-12Rβ1* gene in P1, novel missense homozygous mutation: c.107 A > T/p.Q36L in

* Corresponding author.
** Corresponding author at: Institute of Pathology and Diagnostic Medicine, Khyber Medical University, Peshawar 25000, Pakistan.
E-mail addresses: nadeem.ullah@umu.se (N. Ullah), tajalikhan.ibms@kmu.edu.pk (T.A. Khan).
[1] ORCID ID: https://orcid.org/0009–0008-0149–5988
[2] ORCID ID: https://orcid.org/0000–0003-3074–1953
[3] ORCID ID: https://orcid.org/0000-0002-4165-5738
[4] ORCID ID: https://orcid.org/0000–0002-5933–270X
[5] ORCID ID: https://orcid.org/0000–0003-0339–2487
[6] ORCID ID: https://orcid.org/0000–0003-4011–999X
[7] ORCID: https://orcid.org/0000–0002-2162–3827
[8] ORCID ID: https://orcid.org/0000-0003-1827-3659
[9] ORCID ID: https://orcid.org/0000–00016089-8906

https://doi.org/10.1016/j.jiph.2023.06.005

exon 3 of the *STAT1* gene in P2, missense hemizygous mutation:: c.950 A > C/p.Q317P in exon 8 of the *NEMO* gene in P3, and nonsense hemizygous mutation: c.868 C > T/p.R290X in exon 8 of *CYBB* gene in P4.
Conclusion: Our findings broaden the clinical and genetic spectra associated with IL-12/23/ISG15-IFN-γ axis anomalies. Additionally, our data suggest that TB patients in Pakistan should be investigated for potential genetic defects due to high prevalence of parental consanguinity and increased incidence of TB in the country.

1. Introduction

Tuberculosis (TB) is primarily caused by *Mycobacterium tuberculosis* (*M. tuberculosis*), is the second leading cause of deaths worldwide after coronavirus disease-19 (COVID-19). TB is an airborne infectious disease that mainly affects the lungs, globally approximately 10 million cases reported annually. According to the World Health Organization (WHO), South-East Asia, including Pakistan, has the highest incidence of TB cases [1,2]. Mycobacterial infections are frequently documented in patients with human immunodeficiency virus (HIV) and severe forms of primary immunodeficiencies (PIDs), such as severe combined immune deficiency (SCID), CD40 deficiency, nuclear factor kappa-beta essential modulator (*NEMO*) deficiency, chronic granulomatous disease (CGD), hyper IgE syndrome, and defects in the interleukin-12/23IL-12/23/ISG15-IFN-γ circuit [3–5].

Among these PIDs, the IL-12/23/ISG15-IFN-γ circuit is the main immunological pathway for controlling intra-macrophagic pathogens such as *Mycobacteria, Salmonella* and *leishmania* spp [6,7]. The intra-macrophagic infections stimulate the IL-12/23/ISG15-IFN-γ pathway resulting in the activation of intracellular immunity necessary for the control of *Mycobacteria* and other intracellular pathogens [8–10]. Notably, mutations in genes of the IL-12/23/ISG15-IFN-γ pathway result in increased susceptibility to mycobacterial infections; hence, this condition is commonly referred as Mendelian susceptibility to mycobacterial disease (MSMD). Other intracellular pathogens, such as *Salmonella* and *Leishmania* spp, can also cause infections in otherwise healthy people with an IL-12/23/ISG15-IFN-γ pathway malfunction; due to this reason, MSMD is also known as an "inborn error of the IFN-γ pathway"[11–17]. Germline mutations in 18 genes in this pathway (*IL-12Rβ1, STAT1, CYBB, NEMO, IL-12Rβ2, IL12B, IL23R, IFNG, IFNGR1, IFNGR2, ISG15, ZNFX1, IRF8, TBX21, SPPL2A, JAK1, TYK2* , and *RORC*) have been linked to 34 distinct genetic disorders [18–21]. Importantly, mutations in genes (*IL-12Rβ1*, *IL-12Rβ2*, *IRF8*, *ISG15*, and *NEMO*) limit the induction of IFN-γ, whereas mutations in genes (*IFNGR1, IFNGR2, STAT1,* and *CYBB* also known as *NOX2*) eliminate the response to IFN-γ and impaired IFN-γ immunity. As mentioned earlier, IL-12/23/ISG15-IFN-γ pathway abnormalities are related to impaired anti-mycobacterial immune response and causes increase susceptibility to TB [18,19,22–24]. Due to high TB incidence of 259 cases per 100,000 people annually in Pakistan, this is the country's most significant public health concern [25]. In Pakistan, Bacillus Calmette-Guérin (BCG) vaccination is mandatory for all newborns for immunization against TB [26]. Unfortunately, patients with defective IL-12/23/ISG15-IFN-γ pathway can develop BCG adverse reactions as BCG is a live attenuated vaccine [27].

Considering that inborn error of the IFN-γ pathway can result in TB susceptibility [27–30], therefore, the purpose of this study was to characterize the functional integrity of IL-12/23/ISG15-IFN-γ pathway in individuals with TB-related PID. The characterization of immunological defects of TB patients is essential because clinical outcomes and therapeutic responses depend on the type of defects that impair IFN-γ immunity (either by preventing IFN-γ production or by inducing aberrant responses to IFN-γ).

2. Materials and methods

Relevant clinical information, such as previous TB family history, parental consanguinity, BCG complications, and TB (confirmed by the GeneXpert MTB/RIF and culture technique), was obtained from all HIV-negative patients. Consent forms signed by the patients, or their parents, were obtained, and whole blood samples were collected and processed accordingly. The ethical board of Khyber Medical University, Peshawar, Pakistan, approved this study via letter No. DIR/KMU-EB/FG/000673.

2.1. Separation of peripheral blood mononuclear cells (PBMCs)

From 10 ml of heparinized whole blood collected from patients and healthy controls, PBMCs were separated using Ficoll-Paque density gradient centrifugation as per recommended protocol with minor modification. [28]. Briefly, 10 ml of Ficoll Paque (1.077 ± 0.001 g/ml) was added to 50 ml of falcon tubes (Corning, NY, Mexico) before 10 ml of blood from the patients and healthy donors were carefully layered on top. After 30 min of density gradient centrifugation at 800 g, the interface layer containing PBMCs were collected in another 50 ml of falcon tube and washed twice with phosphate buffered saline (PBS). The PBMCs were enumerated and utilized in various immunological tests.

2.2. IL-12 and IFN-γ cytokines assessment through Enzyme-Linked Immunosorbent Assay (ELISA)

PBMCs from patients and healthy controls were stimulated with BCG + IFN-γ and BCG + IL-12 accordingly [27] The ELISA technique was used to determine IL-12 and IFN-γ cytokines levels using ELISA kits (STEMCELL Technologies).

2.3. Evaluation of IFN-γR1 and IL-12Rβ1 receptor surface expression on Monocytes and T lymphocytes

The surface expression of the IL-12Rβ1 receptor on T lymphocytes was measured using flow cytometry as previously explained [27]. Briefly, PBMCs were stimulated for three days with 8 μg/ml of phytohemagglutinin (PHA) in order to induce IL-12Rβ1, followed by staining with anti-Human IL12Rβ1/CD212 antibody (Extracellular Domain., PE, LifeSpan Bio-Sciences., Inc). Flow cytometry was performed on cells treated with 2% paraformaldehyde using a BD FACS Canto II cytometer (BD Biosciences, San Diego, California, United States) and FlowJo software (TreeStar, Ashland, Oregon) for data processing. Similarly, PBMCs were stained with anti-Human CD119/IFN gamma receptor 1, and gated monocytes on FSC/SSC were analyzed for IFNγR1.

2.4. Detection of STAT1 and STAT4 phosphorylation

Detection of STAT1/STAT4 phosphorylation was performed on monocytes and T lymphocytes after stimulation with recombinant human IFN-γ (rhIFN-γ) and recombinant human IL-12 (rhIL-12)

respectively, as described previously [27]. Staining with an anti-pTyr701-STAT1/anti-pY693-STAT4 antibody (BD Bio-sciences) was performed after fixation and permeabilization. The flow cytometric analysis of *STAT1/STAT4* phosphorylation was performed in gated monocytes, and T lymphocytes, respectively, and the phosphorylation was assessed by the FlowJo software (Treestar, Inc., Ashland., Ore.,).

2.5. Flow cytometric analysis of oxidative burst and NADPH oxidase components

The capacity of neutrophils to induce oxidative burst (H2O2) was measured as described previously with minor modifications [28]. 200 μL of heparinized whole blood (patients and healthy control) was stimulated with phorbol myristate acetate (PMA 300 ng/ml), (Sigma Laboratories, St. Louis, MO, USA) for 20 min, followed by incubation at 37 degrees Celsius for 5 min with dihydrorhodamine 123 (DHR-123) (Sigma-Aldrich). After erythrocytes lysis with RBC lysis solution at 25 °C for 10 min and the cells were washed twice with PBS, 1% paraformaldehyde was used to fix the cells. Neutrophils were gated using flow cytometry (BD FACSCanto II), and H2O2 was quantified on neutrophils using the FlowJo software (Treestar, Inc., Ashland, Ore). As previously described, the membrane bound NOX2 protein of the NADPH oxidase complex was assessed by flow cytometry [28]. Anti-NOX2 antibody (Mouse IgG, k; BioLegend Inc.) was applied to neutrophils, and flow cytometric analysis was performed to detect membrane bound NOX2 protein.

2.6. NEMO expression and degrade IκB-α analysis

For the staining of NEMO in monocytes, PBMCs (2×10^5) were fixed with 2% paraformaldehyde and permeabilized as described previously [31,32]. Briefly, for intracellular staining of *NEMO*, the cells were incubated with anti-NEMO antibodies and then washed twice with PBS. Flow cytometry was used to evaluate intracellular *NMEO* expression in monocytes from patients and healthy controls. The degradation of *IκB*-α was carried out as previously described with minor modification [29]. Briefly, PBMCs of the patient and healthy controls were subsequently treated with TNF-α, and ionomycin calcium ionophore. The 2% paraformaldehyde was used to fix the cells, and the degradation of IκB-α was assessed by flow cytometry.

2.7. Mutational analyses of IL-12Rβ1, STAT1, NEMO and CYBB genes

Wizard® genomic DNA purification kit (Promega) was used for extraction of Genomic DNA from EDTA-chelated blood. Full exons of *IL-12Rβ1, STAT1, NEMO* and *CYBB* genes were amplified by PCR using specific primers (forward and reverse) for each exon. PCR products were sequenced on ABI 3730xl DNA Sequencer and mutational sequence analysis were performed on biological sequence alignment editor (BioEdit) tool.

2.8. Prediction of possible impact of amino acid substitutions on the structure and function of IL-12Rβ1, STAT1, NEMO and CYBB proteins

MutationTaster was used to predict the pathogenicity of novel mutations. The comparative three-dimensional (3D) structures of wild-type and mutant (IL-12Rβ1, STAT1, NEMO and CYBB) proteins were constructed based on the crystal structures. Utilizing program MODELLER 9v15, the structures (3D) of mutants and their wild-type counterparts were compared, and the top models were selected using the PROCHECK and ProSa evaluation procedures. Multiple sequence alignment was performed with ClustalW2 (https://www.ebi.ac.uk/Tools/msa/clustalw2/).

2.9. Data analysis

The GraphPad Prism 8 statistical software (GraphPad Software, San Diego, CA) was used to analyze the obtained data.

3. Results

3.1. Clinical presentations of P1, P2, P3 and P4

The P1 presented with BCG lymphadenitis after BCG vaccination when she was just two months old and pneumonia at the age of one year, and her recovery took three weeks at hospital. At the age of fifteen years, she was diagnosed with TB, and the treatment took more than ten months to recover despite *M. tuberculosis* being drug sensitive. At the age of 17 years, she was infected with severe Cutaneous leishmaniasis on her left leg. Her lesion did not improve with anti-leishmanial treatment and took six months to recover. The P2 developed severe viral pneumonia after her birth and was hospitalized for one month. She did not produce any BCG complications, and later on, at the age of four, she complained of severe chest and throat infections and responded well to treatment. At the age of 10 years, she was diagnosed with severe TB, and her response to anti-tuberculosis was poor. After 12 months of TB, her test was negative for *M. tuberculosis*, later she also developed COVID-19. P3 is male and has typical NEMO deficiency associated with clinical symptoms of ectodermal dysplasia (sparse hair and conical teeth). The P3 had BCG vaccination without BCG complication, and he developed TB at the age of eight, and his response to anti-TB treatment was good. His test after eight months was negative for *M. tuberculosis*. However, at the age of eleven years, he developed TB again but recovered after eight months treatment. The P4 presented BCGitis and severe clinical presentations after birth, such as fever, diarrhea, oral infections, and skin rashes. He tested positive for TB when he was just 12 years of age and was given anti-TB treatment for ten months.

3.2. Evaluation of 12/23/ISG15-IFN-γ pathway in TB patients

TB patients (P1 and P2) belonging to consanguinity and (P3, and P4) to unrelated families were subjected to ELISA to measure IL-12 and IFN-γ cytokines. The PBMCs of the P1 produced a low level of IFN-γ, while PBMCs from P2 and P3 induced an impaired amount of IL-12 production. The PBMCs from P4 demonstrated normal levels of IL-12 and IFN-γ (Fig. 1, E-F).

3.3. Abnormal surface expression of IL-12Rβ1 on T lymphocytes and abolished phosphorylation of STAT4

Following the abnormal level of IFN-γ measured by ELISA, we used flow cytometer to examine the surface expression of IL-12Rβ1 on T lymphocytes from P1 and healthy control, as well as the phosphorylation of STAT4 in response to IL-12 stimulation. We found that P1 lymphocytes demonstrated abolished surface expression of IL-12Rβ1 and reduced phosphorylation of STAT4 as compared to healthy controls (Fig. 2 A-D). Additionally, in response to IFN-γ stimulation, we found normal expression of IFN-γR1 and reduced STAT1 phosphorylation in monocytes from P2 in comparison to healthy controls (Fig. 3 A-D).

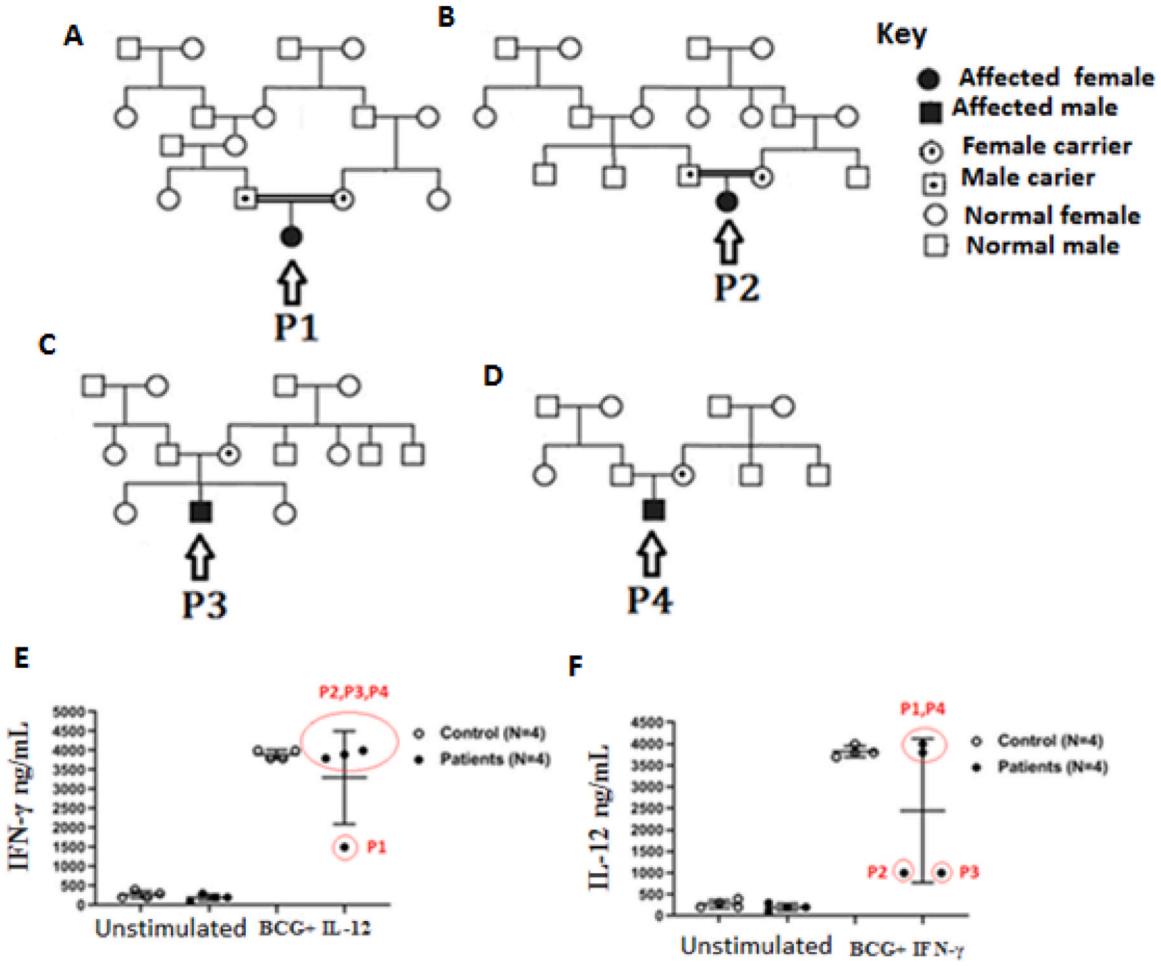

Fig. 1. Family pedigree and functional evolution of IL-12/IFN-γ axis. (A) and (B) filled black circles represent female P1/P2, while (C) and (D) filled black squares represent male P3/P4. Following activation of PBMCs from patients and healthy controls with BCG+IL-12 and IFN- γ + BCG, respectively, (E) and (F) demonstrate the ELISA detection of IFN-γ and IL-12 for all 4 patients (P1, P2, P3 and P4), respectively. Each experiment was conducted independently in triplicate, and a p-value of < 0.005 was considered statistically significant.

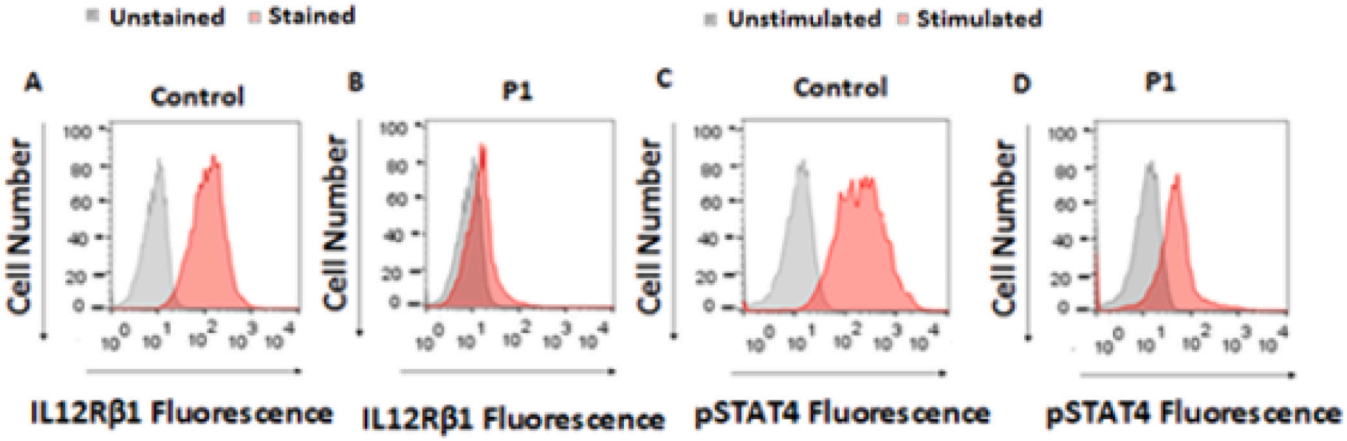

Fig. 2. Flow cytometric analysis of surface expression of IL-12Rβ1 and phosphorylation of STAT4. (A) and (B) black and red filled squares representing unstained and stained with anti-IL-12Rβ1 and demonstrating the surface expression of IL-12Rβ1 on PHA-activated T lymphocytes of healthy control and P1, respectively, and (C) and (D) black and red squares representing the unstimulated and stimulated phosphorylation status in T lymphocytes of healthy control and P1, respectively.

3.4. Reduced degradation of IκB-α displayed by P3 monocytes

We suspected NEMO deficiency based on X-linked pattern, clinical phenotypes such as ectodermal dysplasia (ED), thickened skin, the absence of sweat glands, conical teeth, thin, sparse hair, and susceptibility to infections. We used flow cytometry to examine the intracellular expression of NEMO and degradation of IκB-α in monocytes in response to PMA stimulation. Normal expression of intracellular expression of NEMO and abolished degradation of IκB-α in P3 monocytes were detected (Fig. 4A, B).

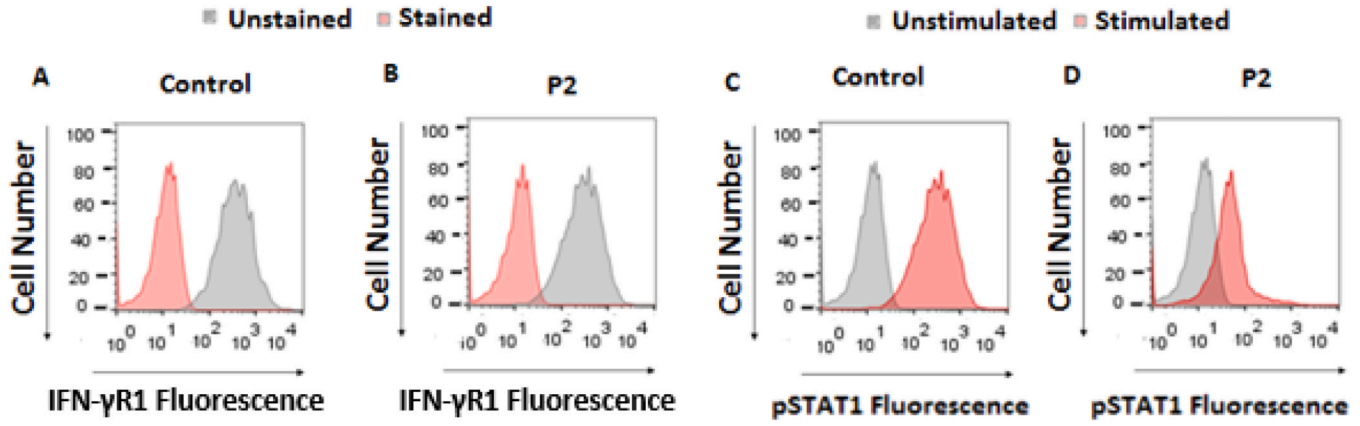

Fig. 3. Flow cytometric evaluation of surface expression of IFN-γR1 and phosphorylation of STAT1. (A) and (B) black and red filled squares represent unstained and stained with anti-IFN-γR1 monocytes and showing surface expression of IFN-γR1 on healthy control and P2 monocytes, respectively, while (C) and (D) black and red filled squares represent unstimulated and stimulated phosphorylation status in healthy control and P2 monocytes, respectively.

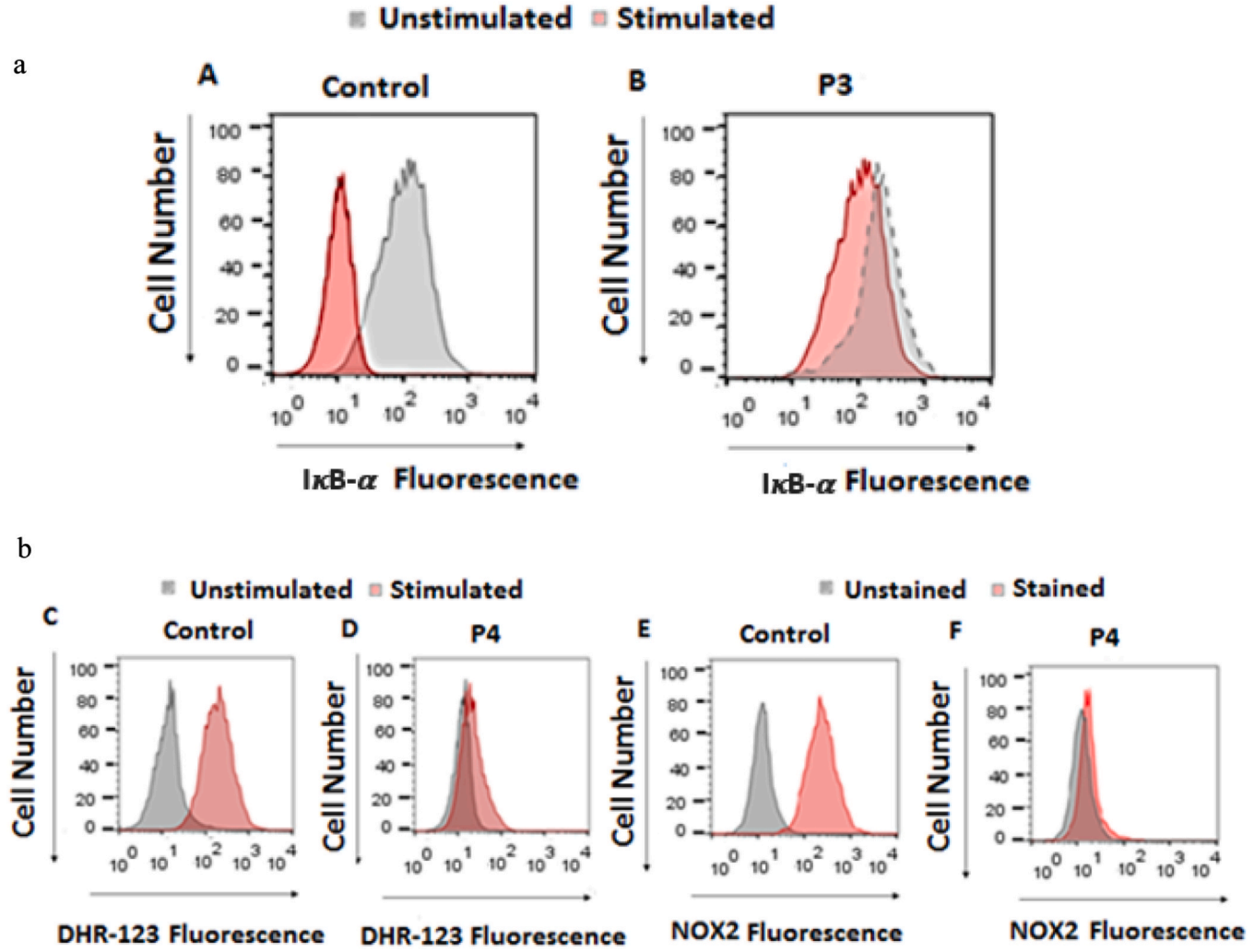

Fig. 4. Flow cytometric analyses of IκB-α degradation, H2O2 production and NOX2 cell membrane protein expression. (A) and (B) filled black and red squares, representing the unstimulated and stimulated status of IκB-α degradation in healthy control and P3 monocytes, respectively. (C) and (D) filled black and red squares, indicating the unstimulated and stimulated levels of H2O2 production in healthy control and P4 neutrophils, respectively, while (E) and (F) filled black and red squares, displaying the unstained and stained with anti-NOX2 and demonstrating the expression of cell membrane protein NOX2 in healthy control and P4 neutrophils.

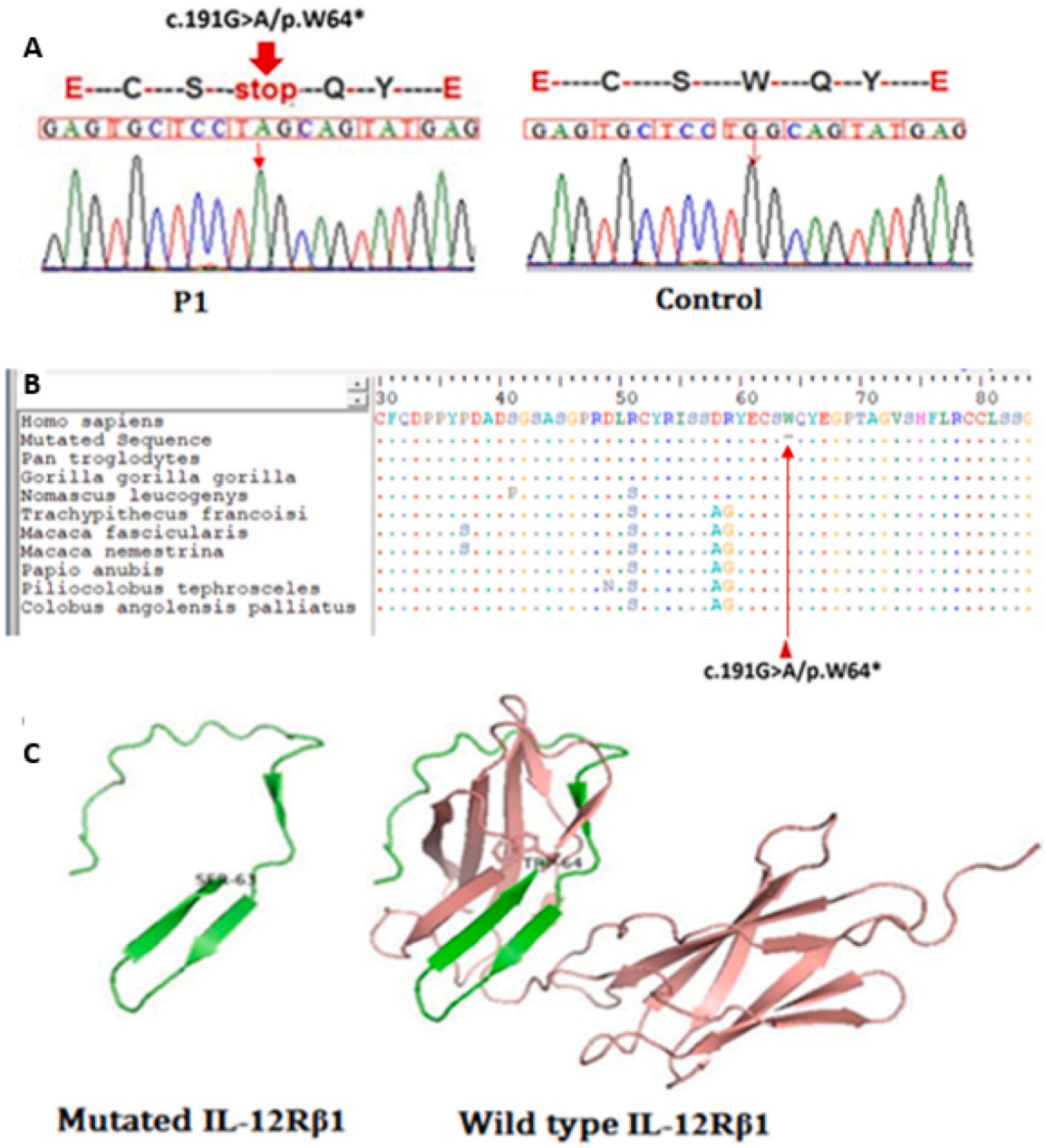

Fig. 5. Genetic and in silico analysis of IL-12Rβ1. (A) and (B) showing the chromatogram of the sequencing of the nonsense mutation: c.191 G > A/p.W64 * in exon 3 of IL-12Rβ1 gene in P1 and the wild-type IL-12Rβ1 gene, respectively, while (B) demonstrates the multiple sequencing alignment of the p.W64 residue across the species and indicates the highly conservation of p.W64. (C) represent 3D mutated and wild-type IL-12Rβ1 proteins, demonstrating that c.191 G > A/p.W64 * resulted in a truncated IL-12Rβ1 protein.

3.5. Reduced oxidative burst and impaired NOX2 by P4 neutrophils

Using flow cytometry, we identified decreased levels of oxidative and NOX2 protein in P4 neutrophils compared to healthy control neutrophils (Fig. 4 C-F).

3.6. Genetic analysis revealed novel mutations in IL-12Rβ1, STAT1, NEMO and CYBB genes

We sequenced the candidate genes based on reduced receptor (IL-12Rβ1), phosphorylation (STAT1/STAT4), IκB-α degradation, and oxidative burst. We found the novel nonsense homozygous mutation: (c.191 G > A/p.W64 *) in exon 3 of the IL-12Rβ1gene in P1, and multiple sequence alignment showed that this p.W64 residue is the same across all the species indicating its conservation. The 3D structural study of wild-type and mutant IL-12Rβ1 indicated that this mutation may result in a truncated IL-12Rβ1 protein (Fig. 5 A, B, C). We also detected a novel a novel homozygous missense mutation, c.107 A > T/p.Q36L, in exon 3 of the STAT1 gene in P2. Multiple sequence alignments reveal that the p.Q36 residue is present in all species, indicating that it is highly conserved. Similarly, the 3D structural analysis of wild-type and mutant *STAT1* predicted that this mutation resulted in a truncated STAT1 protein, which was associated with the abnormal phosphorylation of *STAT1* (Fig. 6A, B, C). We also identified that missense hemizygous mutation: (c.950 A > C/p.Q317P) in exon 8 of NEMO in P3 and nonsense hemizygous

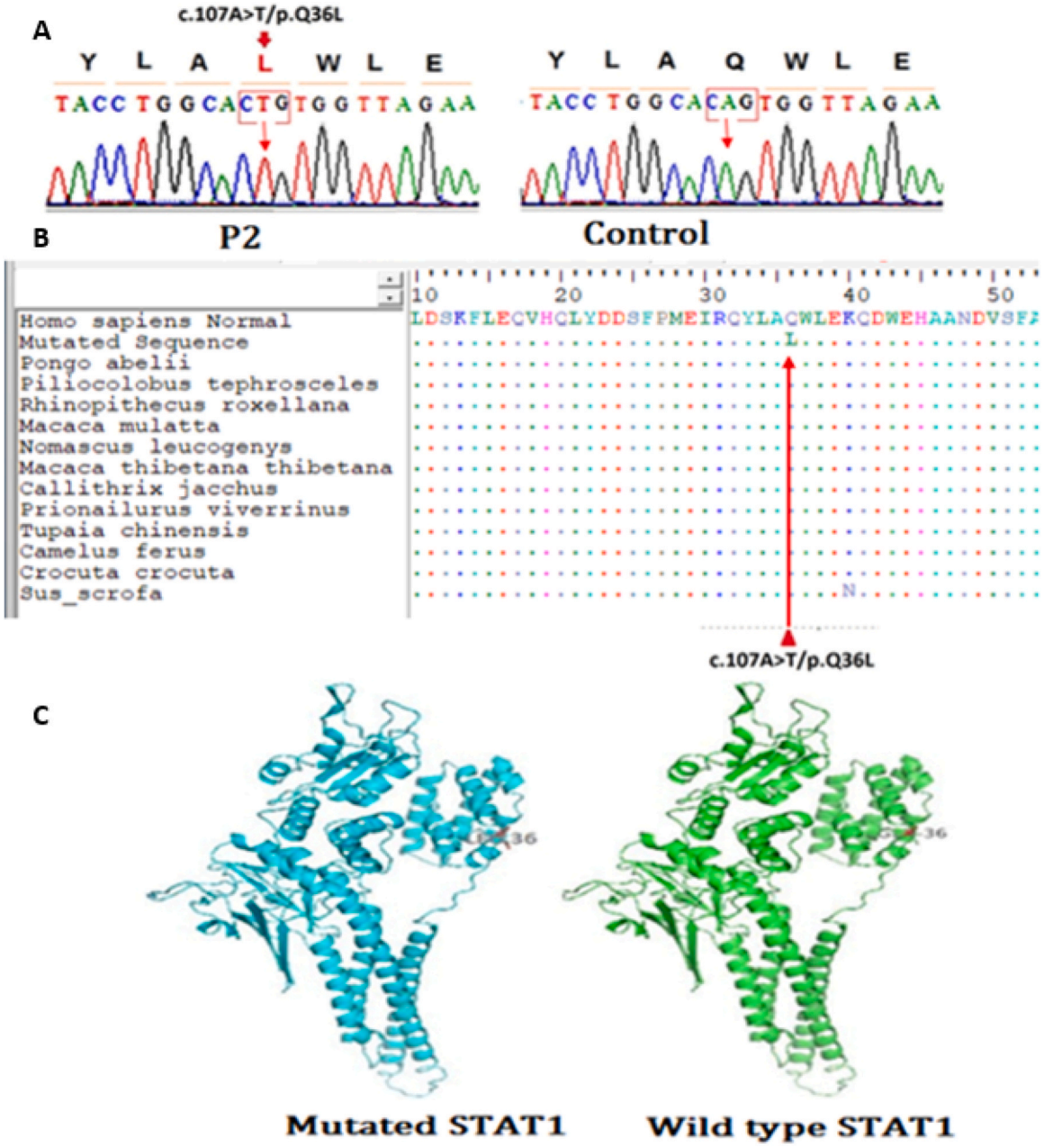

Fig. 6. Genetic and *in silico* analyses of *STAT1*. (A) and (B) showing the chromatogram of the sequencing of a novel missense mutation: c.107 A > T/p.Q36L, in exon 3 of the *STAT1* gene in P2 and the wild-type *STAT1* gene, respectively. At the same time, (B) represents the multiple sequencing alignment of the p.Q36L residue across the species and highlights that the p.W64 residue is highly conserved. (C) show the 3D mutated and wild-type STAT1 proteins, demonstrating that c.107 A > T/p.Q36L resulted in a truncated STAT1 protein.

mutation: c.868 C > T/p.R290X in exon 8 of the CYBB gene in P4 are highly conserved across species, as shown by multiple sequence alignment. Moreover, 3D structural analyses of both wild-type and mutated NEMO and CYBB (p.Q317P and p.R290X) suggested that these mutations disrupt the NEMO and CYBB proteins (Fig. 7 A, B, C) and that these mutations are pathogenic (Fig. 8A, B, C). Significantly, an in silico study utilizing the MutationTaster predicted that all four new mutations (c.191 G > A/p.W64 *, c.107 A > T/p.Q36L, c.950 A > C/p.Q317P, and c.868 C > T/p.R290X) were disease-causing (Fig. 9 A-D).

4. Discussion

In this study, we identified novel mutations in the *IL-12Rβ1, STAT1, NEMO, and CYBB* genes of the IL-12/23/ISG15-IFN-γ axis in patients with severe TB and other infections for the first time. The female P1 developed BCG lymphadenitis, pneumonia, and TB, and the female P2 developed severe viral pneumonia and TB without any BCG complications. At the same time, the male P3 showed signs of typical ectodermal dysplasia, such as sparse hair, conical teeth, and, later, recurrent TB. Male P4 was early stage infected with BCGitis and presented with severe clinical presentations such as fever, diarrhea, oral infections, skin rashes, and severe recurrent TB. So far, using immunological and molecular techniques, we have identified two novel hemizygous mutations (c,191 G > A/p.W64 * in *IL-12Rβ1* and c.868 C > T/p.R290 * in CYBB, and two novel hemizygous missense mutations (c.107 A > T/p.Q36L in STAT1 and c.950 A > C/p.Q317P in *NEMO*). The bioinformatics analyses predicted that these mutations were pathogenic. Although the novel mutations were affecting the

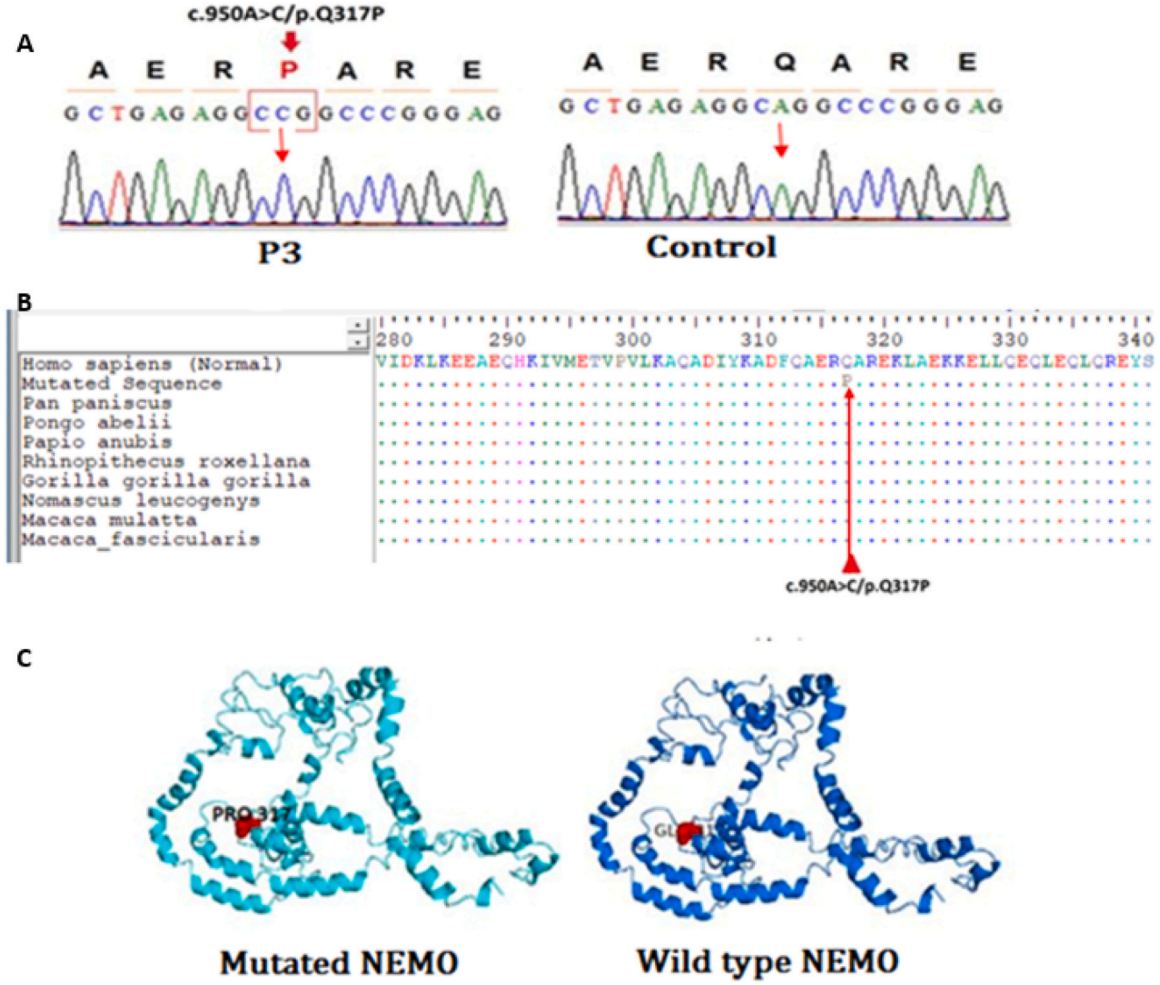

Fig. 7. Genetic and *in silico* analysis of NEMO Protein. (A) and (B) show the chromatogram of the sequencing of a missense mutation: c.950 A > C/p.Q317P in exon 8 of NEMO in P3 and wild type, respectively, while (B) represents the multiple sequencing alignment of the p.Q317 residue across the species and highlights that the p.Q317P residue is highly conserved. (C) shows the 3D mutated and wild-type NEMO proteins and how c.950 A > C/p.Q317P resulted in a truncated NEMO protein.

protein in vitro functionality, however, further characterization would be required, such as site-directed mutagenesis and whole exome sequencing, to declare these novel mutations (c.191 G > A/p.W64 *, c.868 C > T/p.R290 *, c.107 A > T/p.Q36L, and c.950 A > C/p.Q317P) alone pathogenic and responsible for abnormal protein expression and immunological anomalies.

IL-12Rβ1 deficiency is usually associated with BCGitis and intramacrophagic pathogens such as *M. tuberculosis* and *leishmania* [8, 27, 33]. Accordingly, our IL-12Rβ1 deficient P1 developed both BCGitis, TB, and leishmaniasis. This is the third case of cutaneous leishmaniasis associated with a novel IL-12Rβ1 deficiency that we have reported [8]. STAT1 deficiency usually presents both mycobacterial and viral infections [34], and in agreement, STAT1 deficiency in our P2 developed both COVID-19 and TB. NEMO deficiency is associated with several distinct phenotypes, such as abnormal teeth, skin, nails, sweat glands, and hair, and is susceptible to a broad array of infections, including TB [29, 35, 36]. Concurrently, NEMO deficiency in P3 presented typical somatic changes such as sparse hair, conical teeth, and recurrent TB. CYBB deficiency causes increased susceptibility to multiple infections, such as catalase-positive bacterial and mycobacterial infections [28,37–39]. Similar to these findings, the CYBB deficiency in P4 caused increased susceptibility to catalase-positive Staphylococcus aureus and mycobacterial infections (BCGitis and recurrent TB).

According to Global Variome (https://databases.lovd.nl/shared/genes/IL12RB1), up till now, more than 350 variants of IL-12Rβ1 have been reported. We here report a novel nonsense mutation (c.191 G > A/p.W64 *) that causes unknown IL-12Rβ1 deficiency, and this is the fourth novel IL-12Rβ1 deficiency in our group [8,40]. IL-12Rβ1 deficiency is mainly reported in consanguineous families [40–42] and here a novel IL-12Rβ1 defect is also identified in a Pakistani consanguineous family whose parents are carriers of this IL-12Rβ1 deficiency. The novel nonsense mutation, c.191 G > A/p.W64 *, is positioned in exon 3 of the IL-12Rβ1 gene. Currently, six distinct mutations in roughly 12 persons have been identified in exon 3 of the IL-12Rβ1 gene. Therefore, this c.191 G > A/p.W64 * expands the genetic spectrum of high heterogeneous IL-12Rβ1 deficiency. The autosomal recessive form of partial STAT1 deficiency is characterized by poor responses to both IFN-γ and IFN-α/β, increasing susceptibility to intracellular bacterial and viral infections [43]. We only assessed inadequate responses to IFN-γ and did not test the response to IFN-α/β. Therefore, we did not conclude that STAT1 deficiency impaired responses to both IFN-γ and IFN-α/β, although our P2 with STAT1 deficiency developed both viral and mycobacterial diseases.

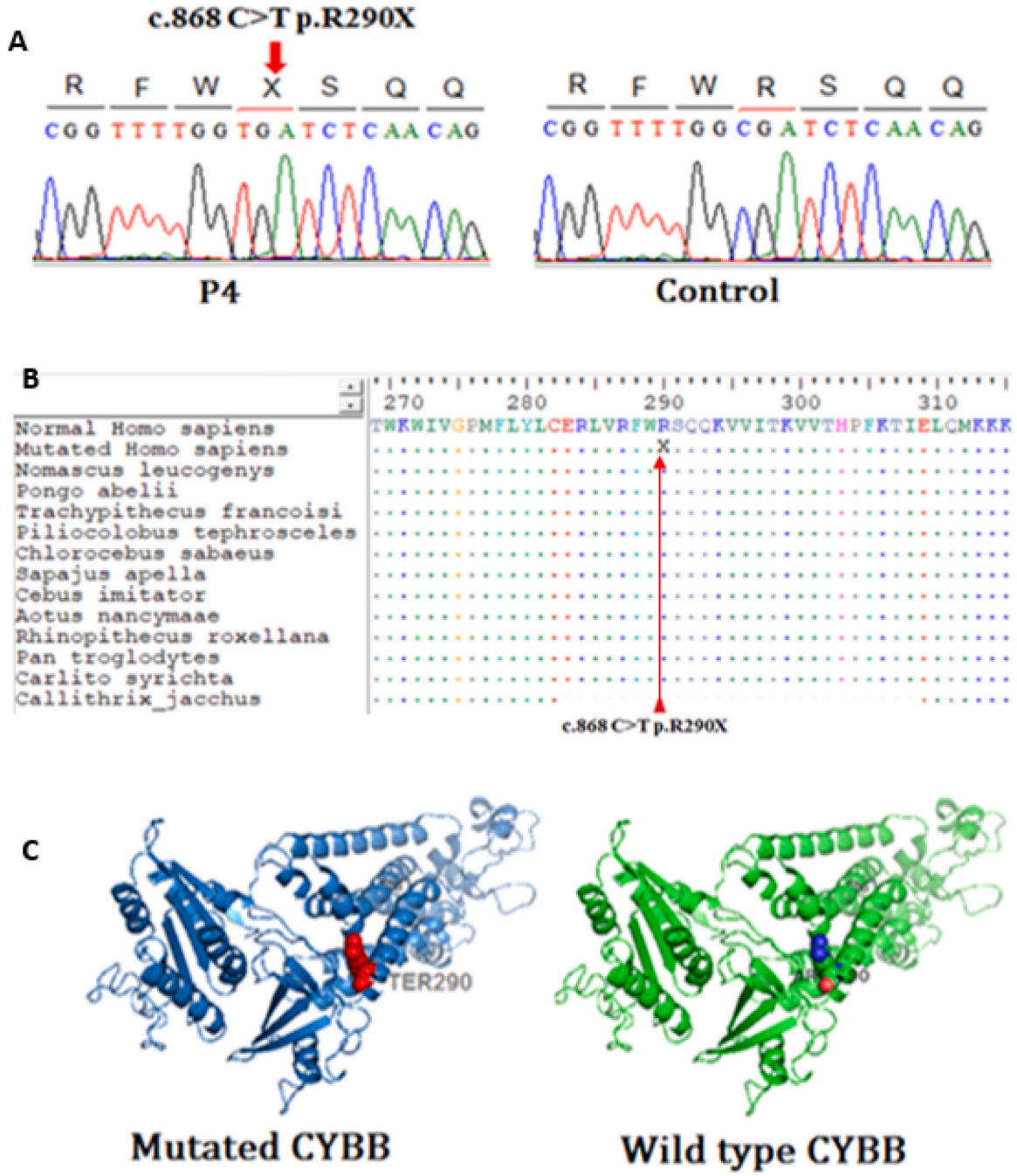

Fig. 8. Genetic and *in silico* analyses of CYBB. (A) and (B) showing the chromatogram of the sequencing of the nonsense mutation: c.868 C > T/p.R290X in exon 8 of the CYBB gene in P4 and wild type, respectively, while (B) represents the multiple sequencing alignment of the p.R290X residue across the species and highlights that the p.R290 residue is highly conserved. (C) representing the 3D mutated and wild-type CYBB proteins and demonstrating that nonsense mutation: c.868 C > T/p.R290X created impaired NEMO protein.

Notably, 32 different NEMO mutations have been reported that caused 80 different phenotypes, of which only 77% developed anhidrotic ectodermal dysplasia with immune deficiency (EDA-ID) [44,45] and are an X-linked recessive disorder (XL-EDA-ID). This is the result of NEMO's hypomorphic mutations. Here, our P3 also presented an XL-EDA-ID phenotype due to a novel missense mutation residing in the leucine zipper domain of NEMO.

Globally, until now, more than 600 mutations have been reported in the CYBB gene that causes X-CGD [37]. Among these mutations, rare nonsense mutations result in a total lack of NOX2 expression (X910CGD), which is associated with altogether abolishing NADPH oxidase activity [46]. In accordance, nonsense mutation: c c.868 C > T/p.R290X caused a variant of X910CGD. The lack of NOX2 expression suggests that this nonsense mutation, c.868 C > T/p.R290X, affects the NADPH oxidase respiratory burst. However, the impact of the mutation: p.R290X on NADPH oxidase assembly requires further characterization using transgenic studies [47]. Our data expand the clinical and genetic spectra associated with the defects of the IL-12/23/ISG15-IFN-γ axis and suggest that TB patients in Pakistan should be evaluated for possible genetic defects due to the high prevalence of parental consanguinity and TB.

4.1. Limitation of the study

The limitation of our study is the site directed mutagenesis and in vivo studies.

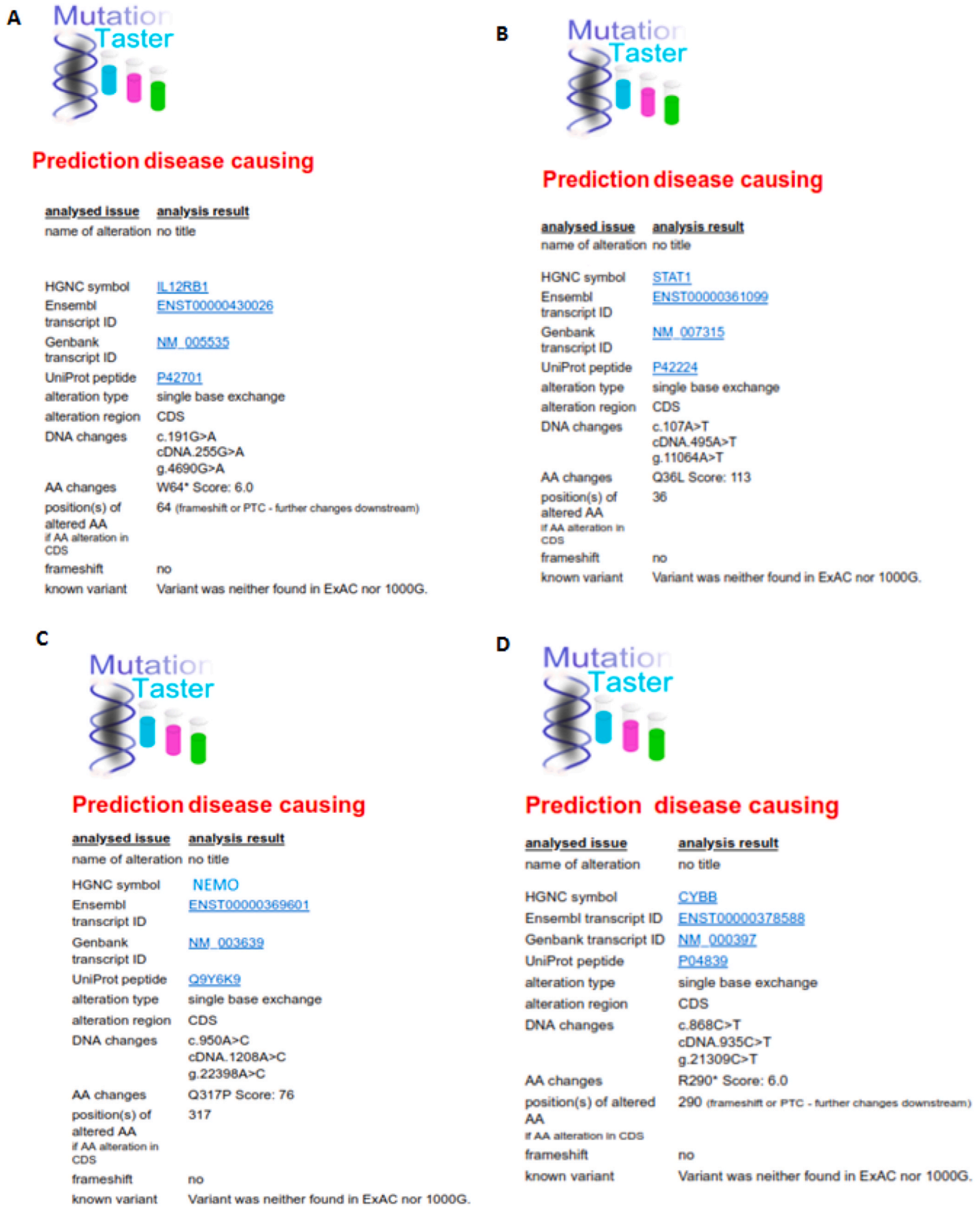

Fig. 9. MutationTaster predictions of mutations. (A, B, C, and D) demonstrating the predictions of the MutationTaster and predicting that all mutations (c.191 G > A/p.mW64 *, c.107 A > T/p.Q36L, c.950 A > C/p.Q317P,and c.868 C > T/p.R290X) are disease-causing.

5. Conclusion

Our findings broaden the clinical and genetic spectra associated with IL-12/23/ISG15-IFN-γ axis anomalies. Additionally, our data suggest that TB patients in Pakistan should be investigated for potential genetic defects due to high prevalence of parental consanguinity and increased incidence of TB in the country.

Declaration of Competing Interest

All authors certify that there are no conflicts of interest.

Acknowledgements

We thank the Jeffrey Modell Foundation of the United States and the Higher Education Commission (HEC) of Pakistan for supporting this project with letter number 10352/KPK/NRPU/R&D/HEC/2017. We also acknowledge ORIC-KMU for providing financial support.

References

[1] Khan AS, Phelan JE, Khan MT, Ali S, Qasim M, Napier G, et al. Characterization of rifampicin-resistant Mycobacterium tuberculosis in Khyber Pakhtunkhwa, Pakistan. Sci Rep 2021;11(1):14194.
[2] W.H.O. Global tuberculosis report 2021. ⟨https://wwwwhoint/teams/global-tuberculosis-programme/tb-reports⟩. 2021.
[3] Ulusoy E, Karaca NE, Aksu G, Çavuşoğlu C, Kütükçüler N. Frequency of Mycobacterium bovis and mycobacteria in primary immunodeficiencies. Turk Pediatri Ars 2017;52(3):138.
[4] Lee PP. Disseminated Bacillus Calmette-Guerin and susceptibility to mycobacterial infections-implications on Bacillus Calmette-Guerin vaccinations. Ann Acad Med Singap 2015;44(8):297–301.
[5] Braue J, Murugesan V, Holland S, Patel N, Naik E, Leiding J, et al. NF-κB essential modulator deficiency leading to disseminated cutaneous atypical mycobacteria. Mediterr. J. Hematol. Infect. Dis. 2015;7:1.
[6] MacLennan C, Fieschi C, Lammas DA, Picard C, Dorman SE, Sanal O, et al. Interleukin (IL)-12 and IL-23 are key cytokines for immunity against Salmonella in humans. J Infect Dis 2004;190(10):1755–7.
[7] Wu U-I, Holland SM, editors. A genetic perspective on granulomatous diseases with an emphasis on mycobacterial infections. Seminars in immunopathology. Springer.; 2016.
[8] Khattak FA, Akbar NU, Riaz M, Hussain M, Rehman K, Khan SN, et al. Novel IL-12Rβ1 deficiency-mediates recurrent cutaneous leishmaniasis. Int J Infect Dis: IJID: Publ Int Soc Infect Dis 2021;112:338–45.
[9] Sabri A, Grant AV, Cosker K, El Azbaoui S, Abid A, Abderrahmani Rhorfi I, et al. Association study of genes controlling IL-12-dependent IFN-γ immunity: STAT4 alleles increase risk of pulmonary tuberculosis in Morocco. J Infect Dis 2014;210(4):611–8.
[10] Taur PD, Gowri V, Pandrowala AA, Iyengar VV, Chougule A, Golwala Z, et al. Clinical and molecular findings in mendelian susceptibility to mycobacterial diseases: experience from India. Front Immunol 2021;12:631298.
[11] Rosenzweig SD, Holland SM. Defects in the interferon-γ and interleukin-12 pathways. Immunol Rev 2005;203(1):38–47.
[12] van de Vosse E, Haverkamp MH, Ramirez-Alejo N, Martinez-Gallo M, Blancas-Galicia L, Metin A, et al. IL-12 R β1 deficiency: mutation update and description of the IL 12 RB 1 variation database. Human Mutat 2013;34(10):1329–39.
[13] Vázquez N, Greenwell-Wild T, Rekka S, Orenstein JM, Wahl SM. Mycobacterium avium-induced SOCS contributes to resistance to IFN-γ-mediated mycobactericidal activity in human macrophages. J Leukoc Biol 2006;80(5):1136–44.
[14] Ottenhoff TH, Verreck FA, Lichtenauer-Kaligis EG, Hoeve MA, Sanal O, van Dissel JT. Genetics, cytokines and human infectious disease: lessons from weakly pathogenic mycobacteria and salmonellae. Nat Genet 2002;32(1):97–105.
[15] Rosain J, Kong XF, Martinez-Barricarte R, Oleaga-Quintas C, Ramirez-Alejo N, Markle J, et al. Mendelian susceptibility to mycobacterial disease: 2014–2018 update. Immunol Cell Biol 2019;97(4):360–7.
[16] Casanova J-L, Abel L. Genetic dissection of immunity to mycobacteria: the human model. Annu Rev Immunol 2002;20(1):581–620.
[17] Tangye SG, Al-Herz W, Bousfiha A, Chatila T, Cunningham-Rundles C, Etzioni A, et al. Human inborn errors of immunity: 2019 update on the classification from the International Union of Immunological Societies Expert Committee. J Clin Immunol 2020;40(1):24–64.
[18] Bustamante J. Mendelian susceptibility to mycobacterial disease: recent discoveries. Hum Genet 2020;139(6–7):993–1000.
[19] Khan TA, Cabral-Marques O, Schimke LF, de Oliveira Jr. EB, Amaral EP, D'Império Lima MR, et al. Tuberculosis in an autosomal recessive case of chronic granulomatous disease due to mutation of the NCF1 gene. Allergol Et Immunopathol 2016;44(3):276–9.
[20] Le Voyer T, Neehus AL. Inherited deficiency of stress granule ZNFX1 in patients with monocytosis and mycobacterial disease. 2021;118:15.
[21] Zhang Q, Bastard P. Inborn errors of type I IFN immunity in patients with life-threatening COVID-19. Science 2020;370(6515).
[22] Mendelian susceptibility to mycobacterial disease: genetic, immunological, and clinical features of inborn errors of IFN-γ immunity. In: Bustamante J, Boisson-Dupuis S, Abel L, Casanova J-L, editors. Seminars in Immunology. Elsevier; 2014.
[23] Inborn errors of IL-12/23-and IFN-γ-mediated immunity: molecular, cellular, and clinical features. In: Filipe-Santos O, Bustamante J, Chapgier A, Vogt G, de Beaucoudrey L, Feinberg J, editors. Seminars in Immunology. Elsevier; 2006.
[24] Rosenzweig SD, Holland SM. Defects in the interferon-γ and interleukin-12 pathways. Immunol Rev 2005;203(1):38–47.
[25] W.H.O. Global Tuberculosis Control Report 2021. Geneva, Switzerland: World Health Organization; 2021.
[26] Sarfraz Z, Sarfraz A, Pandav K, Singh Makkar S, Hasan Siddiqui S, Patel G, et al. Variances in BCG protection against COVID-19 mortality: A global assessment. J Clin Tuberc Other Mycobact Dis 2021;24:100249.
[27] Ul Akbar N, Khan SN, Amin MU, Ishfaq M, Cabral-Marques O, Schimke LF, et al. Novel nonsense IL-12Rβ1 mutation associated with recurrent tuberculosis. Immunol Res 2019;67(4–5):408–15.
[28] Khan TA, Kalsoom K, Iqbal A, Asif H, Rahman H, Farooq SO, et al. A novel missense mutation in the NADPH binding domain of CYBB abolishes the NADPH oxidase activity in a male patient with increased susceptibility to infections. Microb Pathog 2016;100:163–9.
[29] Khan TA, Schimke LF, Amaral EP, Ishfaq M, Barbosa Bonfim CC, Rahman H, et al. Interferon-gamma reduces the proliferation of M. tuberculosis within macrophages from a patient with a novel hypomorphic NEMO mutation. Pediatr Blood Cancer 2016;63(10):1863–6.
[30] Möller M, Nebel A, van Helden PD, Schreiber S, Hoal EG. Analysis of eight genes modulating interferon gamma and human genetic susceptibility to tuberculosis: a case-control association study. BMC Infect Dis 2010;10:154.
[31] Filipe-Santos O, Bustamante J, Haverkamp MH, Vinolo E, Ku CL, Puel A, et al. X-linked susceptibility to mycobacteria is caused by mutations in NEMO impairing CD40-dependent IL-12 production. J Exp Med 2006;203(7):1745–59.
[32] Nishikomori R, Akutagawa H, Maruyama K, Nakata-Hizume M, Ohmori K, Mizuno K, et al. X-linked ectodermal dysplasia and immunodeficiency caused by reversion mosaicism of NEMO reveals a critical role for NEMO in human T-cell development and/or survival. Blood 2004;103(12):4565–72.
[33] Xie N, Jiang LP, Kong XF, Zhu CM, Liu ZY, Liu W, et al. [Primary immunodeficiency complicated with Bacillus Calmette-Guerin infection: identification and clinical phenotype of a case of novel interleukin-12Rbeta1 gene mutation]. Zhonghua er ke za zhi Chin J Pediatr 2008;46(8):601–4.
[34] Chapgier A, Kong XF, Boisson-Dupuis S, Jouanguy E, Averbuch D, Feinberg J, et al. A partial form of recessive STAT1 deficiency in humans. J Clin Investig 2009;119(6):1502–14.
[35] Priolo M, Laganà C. Ectodermal dysplasias: a new clinical-genetic classification. J Med Genet 2001;38(9):579–85.
[36] Tangye SG, Al-Herz W, Bousfiha A, Cunningham-Rundles C, Franco JL, Holland SM, et al. Human inborn errors of immunity: 2022 update on the classification from the international union of immunological societies expert committee. J Clin Immunol 2022;42(7):1473–507.
[37] Zhang J, Fan M. Identification of a novel mutation in CYBB gene in a Chinese neonate with X-linked chronic granulomatous disease: a case report. Medicine 2022;101(10):e28875.
[38]. Journal of clinical immunology.
[39] Baba LA, Ailal F, El Hafidi N, Hubeau M, Jabot-Hanin F, Benajiba N, et al. Chronic granulomatous disease in Morocco: genetic, immunological, and clinical features of 12 patients from 10 kindreds. J Clin Immunol 2014;34(4):452–8.
[40] Ul Akbar N, Khan SN, Amin MU, Ishfaq M, Cabral-Marques O, Schimke LF, et al. Novel nonsense IL-12Rbeta1 mutation associated with recurrent tuberculosis. Immunol Res 2019;67(4–5):408–15.
[41] de Oliveira-Junior EB, Zurro NB, Prando C, Cabral-Marques O, Pereira PV, Schimke LF, et al. Clinical and genotypic spectrum of chronic granulomatous disease in 71 Latin American patients: first report from the LASID registry. Pediatr Blood Cancer 2015;62(12):2101–7.
[42] Boisson-Dupuis S, El Baghdadi J, Parvaneh N, Bousfiha A, Bustamante J, Feinberg J, et al. IL-12Rβ1 deficiency in two of fifty children with severe tuberculosis from Iran, Morocco, and Turkey. PloS One 2011;6(4):e18524.
[43] Le Voyer T, Sakata S, Tsumura M, Khan T, et al. Immunological, and clinical features of 32 patients with autosomal recessive STAT1 deficiency. J Immunol 2021;207(1):133–52.
[44] Fusco F, Pescatore A, Bal E, Ghoul A, Paciolla M, Lioi MB, et al. Alterations of the IKBKG locus and diseases: an update and a report of 13 novel mutations. Hum Mutat 2008;29(5):595–604.
[45] Bret Puvilland C, Boisson B, Fusaro M, Bustamante J, Bertrand Y, Ceraulo A, et al. EDA-ID: a severe clinical presentation associated with a new IKBKG mutation. J Clin Immunol 2021;41(5):1099–102.
[46] Stasia MJ, Bordigoni P, Floret D, Brion JP, Bost-Bru C, Michel G, et al. Characterization of six novel mutations in the CYBB gene leading to different sub-types of X-linked chronic granulomatous disease. Hum Genet 2005;116(1–2):72–82.
[47] Bionda C, Li XJ, van Bruggen R, Eppink M, Roos D, Morel F, et al. Functional analysis of two-amino acid substitutions in gp91 phox in a patient with X-linked flavocytochrome b558-positive chronic granulomatous disease by means of transgenic PLB-985 cells. Hum Genet 2004;115(5):418–27.